Supporting Information

Selective uptake of rare earths from aqueous solutions by EDTA-functionalized magnetic and nonmagnetic nanoparticles

David Dupont, Ward Brullot, Maarten Bloemen, Thierry Verbiest, Koen Binnemans*

1. DLS measurements

Dynamic light scattering (DLS) measurements were carried out on a Brookhaven 90plus particle analyzer with the scattering angle set at 90°. DLS measures the hydrodynamic radii and the polydispersity of the nanoparticles. The hydrodynamic radius is that of a sphere with the same translational diffusion coefficient as the particle being measured. It takes into account the solvent layer moving together with the particle. The β-value represents the polydispersity of the nanoparticles. A β of 1 indicates very monodisperse nanoparticles and a β of 0.6 indicates a rather polydisperse sample. The β-value is an interesting indicator for aggregation in solution. An increase in hydrodynamic radius with pH confirmed that the solvation shell increases with increasing surface charge or zeta potential. The β close to 1 confirmed the limited aggregation in solution.

Table S 1. DLS results showing the hydrodynamic radius as function of charge per EDTA group.

	pH	Charge per SG[(a)]	Hydrodynamic diameter (nm)	β-value[(c)]
Fe_3O_4(TMS-EDTA)	10.5	-3	68.2	0.95
Fe_3O_4(TMS-EDTA)	7.0	-2	65	0.95
Fe_3O_4(TMS-EDTA)	4.5	-1	61.8	0.96
Fe_3O_4(TMS-EDTA:Ho)	6.5	0	55.4	0.90
Fe_3O_4(NOA)	6.0	/	51.8	0.95

(a) Approximate charge per surface group based on the pK_a values (see paper)
(b) Polydispersity index (β = 1 indicates monodisperse β = 0.6 is polydisperse).

2. IR measurements

Fourier Transform Infrared (FTIR) spectra were measured between 4000 and 500 cm^{-1} on a Bruker Vertex 70 spectrometer, with a Platinum ATR module. The spectra of the three functionalized nanoparticles Fe_3O_4(TMS-EDTA), TiO_2(TMS-EDTA) and SiO_2(TMS-EDTA) are shown versus the unfunctionalized nanoparticle (Fe_3O_4, TiO_2 and SiO_2). Fe_3O_4 nanoparticles are very unstable so the oxide powder was used instead.

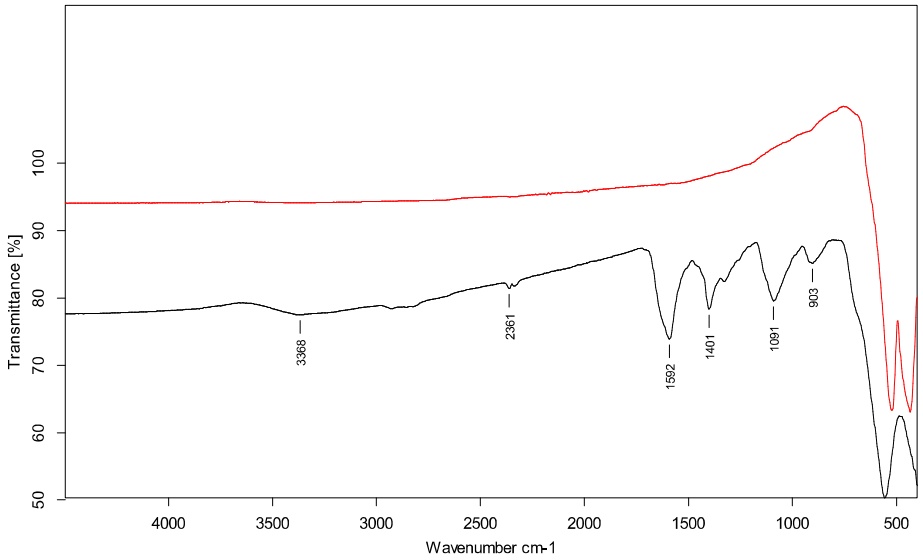

Figure S1. FTIR spectrum of Fe_3O_4(TMS-EDTA) (black line) and Fe_3O_4 oxide (red line).

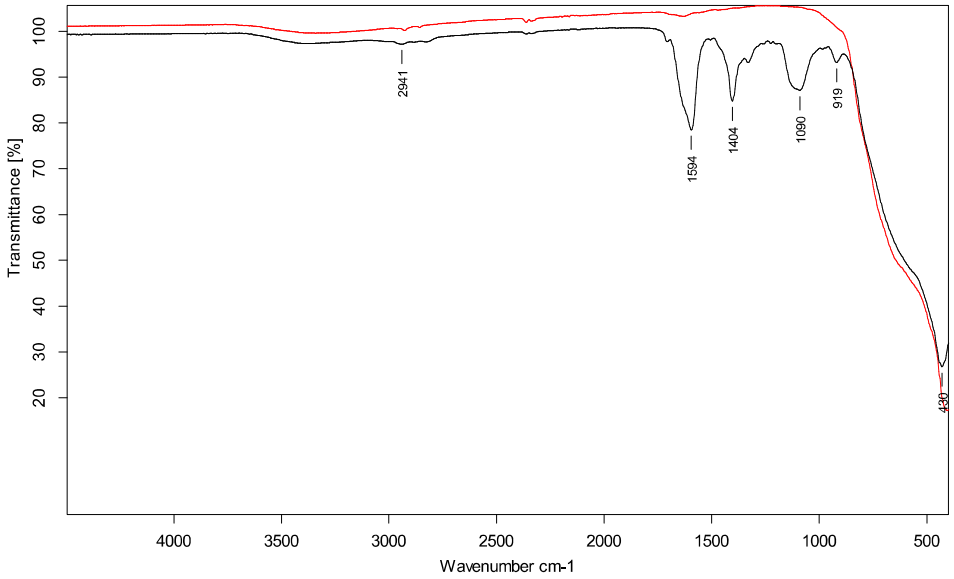

Figure S2. FTIR spectrum of TiO_2(TMS-EDTA) (black line) and TiO_2 (red line) nanoparticles.

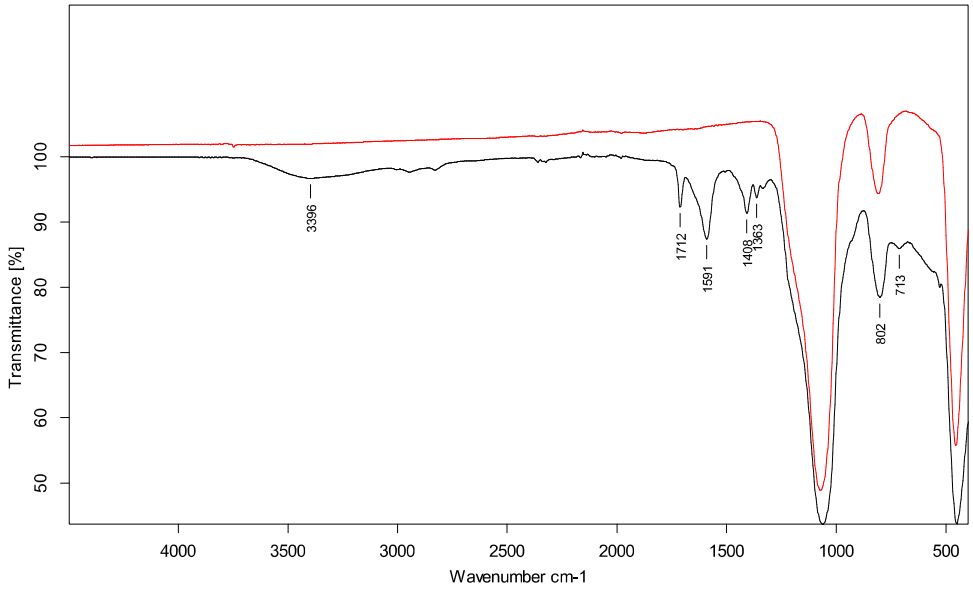

Figure S3. FTIR spectrum of SiO_2(TMS-EDTA) (black line) and SiO_2 (red line) nanoparticles.

3. Vibrating Sample Magnetometry (VSM) measurements

The magnetization versus applied magnetic field loop was obtained by Vibrating Sample Magnetometry (VSM) measurements at 300 K. The magnetic nanoparticles had a saturation magnetization of 66 emu/g and negligible coercivity and remanent magnetization, indicating superparamagnetic behavior.

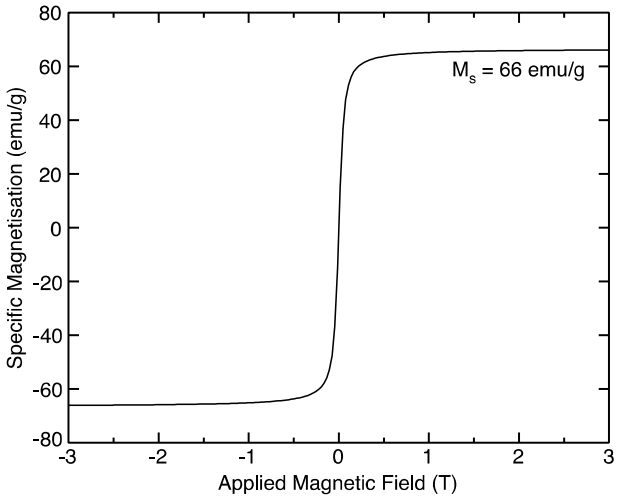

Figure S4. VSM measurement for Fe_3O_4(TMS-EDTA) nanoparticles.

4. TEM measurements

Transmission electron microscopy (TEM) measurements were carried out on a JEOL JEM2100 apparatus using an acceleration voltage of 80 kV or 200 kV. The diameter of the nanoparticles was measured using ImageJ software in order to determine the average size, standard deviation and size distribution.

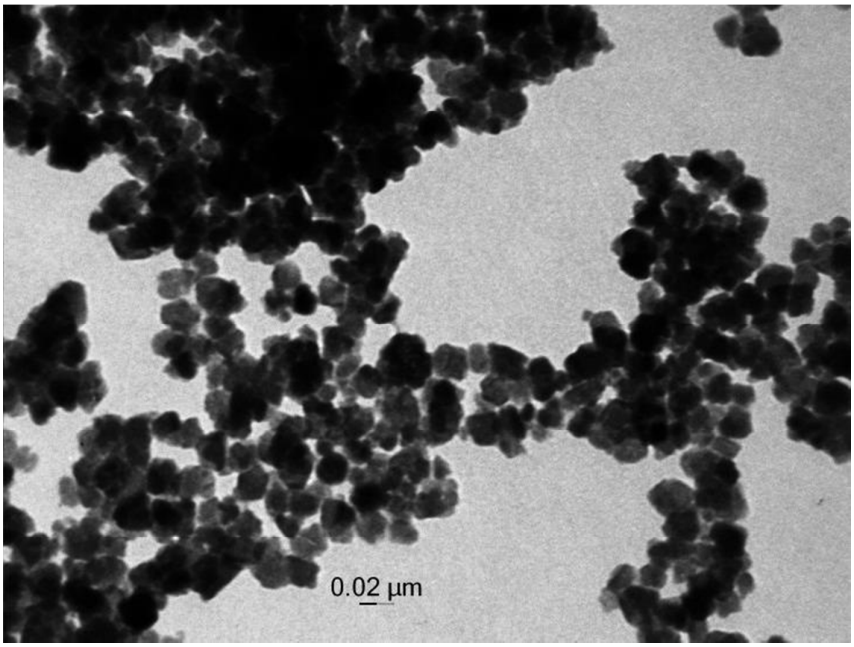

Figure S5. TEM image of Fe_3O_4(TMS-EDTA).

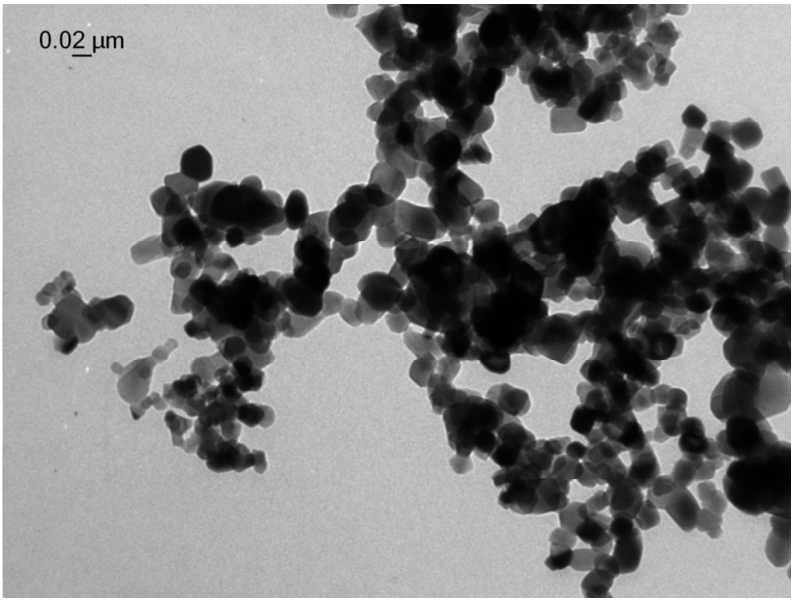

Figure S6. TEM image of TiO_2(TMS-EDTA).

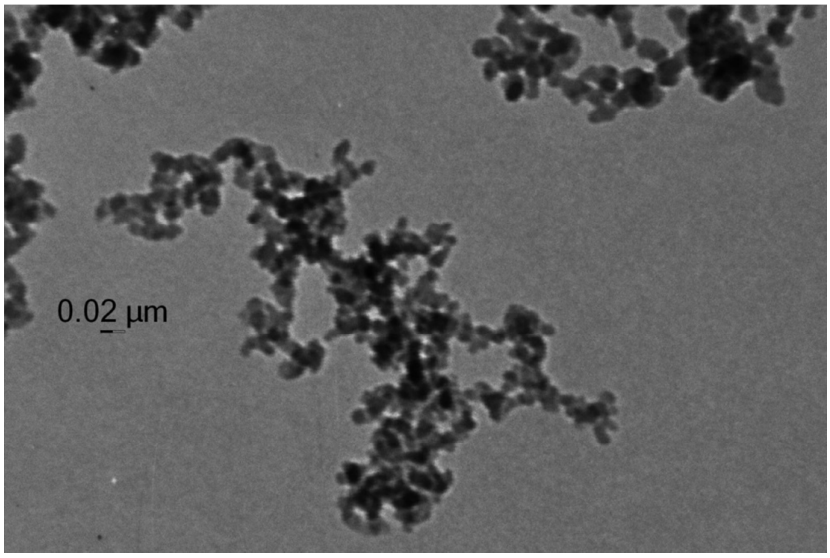

Figure S7. TEM image of SiO_2(TMS-EDTA).

5. Thermogravimetric analysis (TGA)

Thermogravimetric (TGA) analysis was used to determine the amount of functional groups attached to the surface of the nanoparticles (*Figure S**8***). The TGA curves of unfunctionalized SiO_2 and TiO_2 nanoparticles were added for comparison.

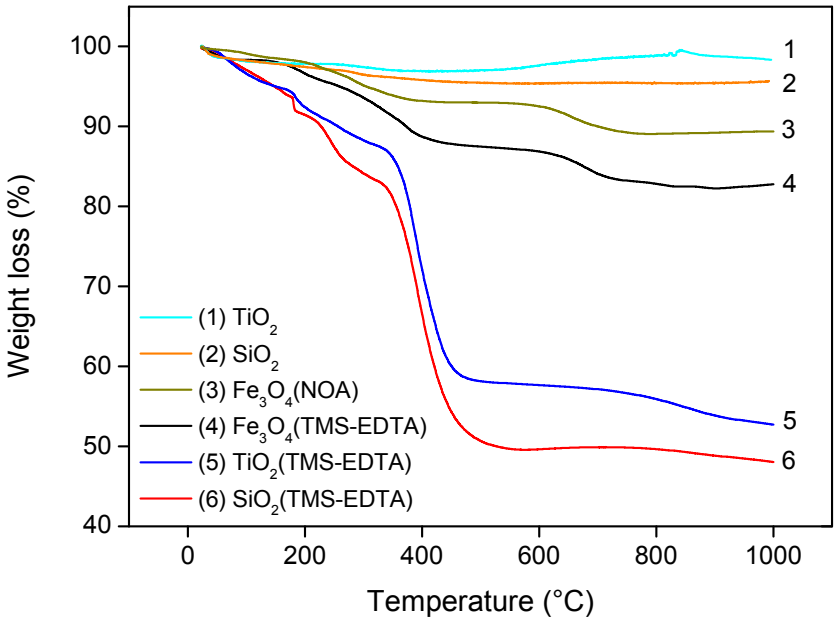

Figure S8. TGA curves (10°C/min under argon) of the different nanoparticles.

6. Zeta potential as function of pH

The zeta potential was measured on a Brookhaven 90plus particle analyzer at different pH values using an HCl solution. The zeta potential is a measure for the electrostatic stabilization of the nanoparticles in solution. The point of zero charge (PZC) is situated around pH 2.8.

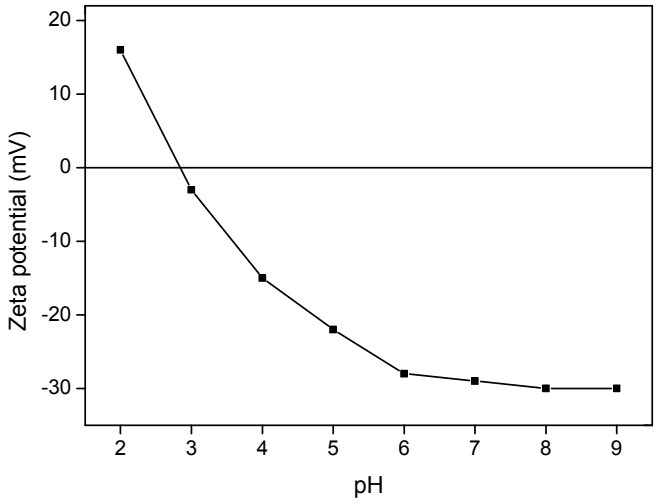

Figure S9. Zeta potential as function of pH for Fe_3O_4(TMS-EDTA) nanoparticles.

7. Verifying the absence of precipitation below pH 6.5

The adsorption experiments were only valid up to pH 6.5 because after this pH the ions precipitate. This is shown in Figure S10 were the sudden precipitation at pH > 6.5 is clearly visible. Between pH 3 and 6.5 the increase in adsorption is attributed to the increasingly deprotonated EDTA groups.

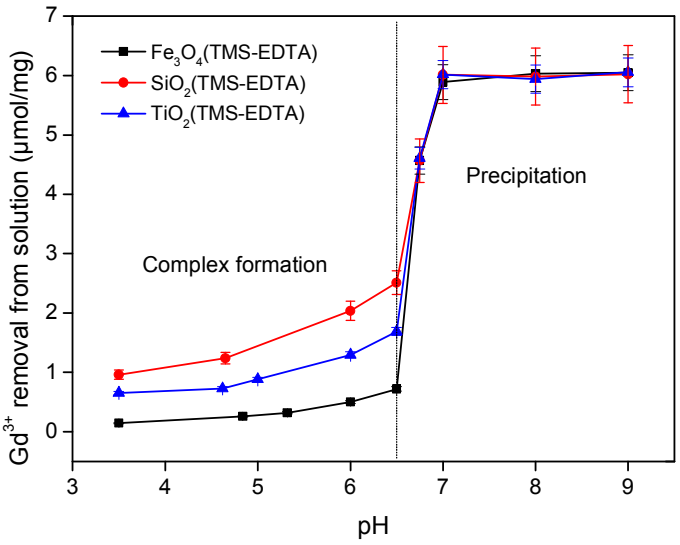

Figure S10. Removal of Gd^{3+} from solution as function of pH.

8. Using an excess of rare-earths

It is necessary to use an excess of rare-earth ions compared to the amount of EDTA present on the nanoparticles in solution. If this condition is not met, the EDTA groups will adsorb all the ions in solution without much selectivity. Selectivity is observed when an excess of (binary) solutions of rare-earths is added (REE/EDTA molar ratio > 1).

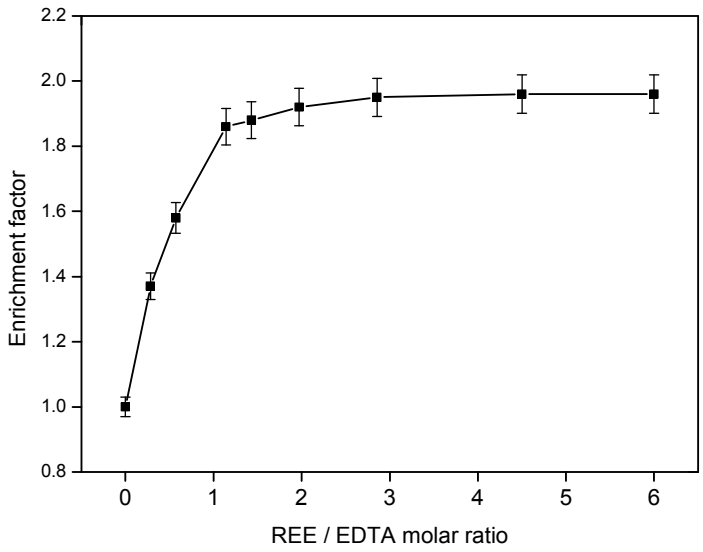

Figure S11. Separation of a Ho^{3+}/Y^{3+} (1:1) solution with Fe_3O_4(TMS-EDTA) nanoparticles. The enrichment of Ho^{3+} over Y^{3+} is shown as function of the molar ratio between the rare-earth ions (REE) and the immobilized silane-EDTA groups in solution.

9. The influence of the counter ion on the separation

The influence of the counter ion on the selectivity was investigated by carrying out extraction experiments with Fe_3O_4(TMS-EDTA) nanoparticles on chloride and nitrate rare-earth pairs at pH 6.5. No significant effect was observed, which is why the nitrate salts were used in all experiments. The chloride salts for this specific experiment, were purchased from following suppliers: $LaCl_3 \cdot 7H_2O$ (99.9%) and $PrCl_3 \cdot 6H_2O$ (99.9%) from Acros Chemicals, $NdCl_3 \cdot 6H_2O$ (99.9%), $YCl_3 \cdot 6H_2O$ (99.9%), $SmCl_3 \cdot 6H_2O$ (99.9%), $GdCl_3 \cdot 6H_2O$ (99.9%), $DyCl_3 \cdot 6H_2O$ (99.9%), and $HoCl_3 \cdot 6H_2O$ (99.9%) from Alfa Aesar. All chemical were used as received without further purification.

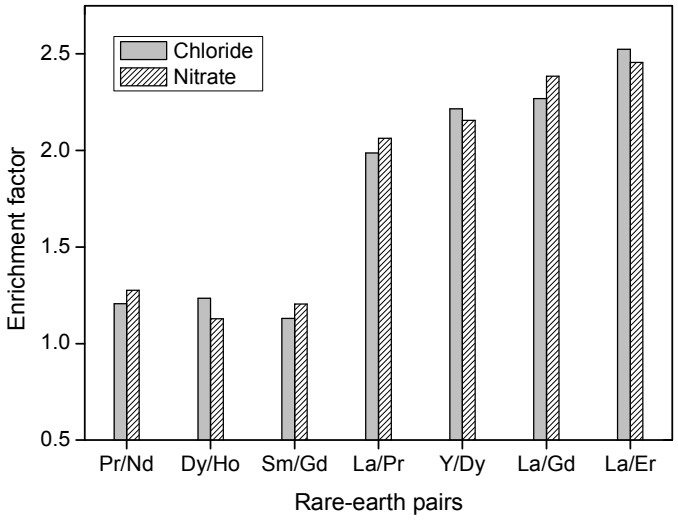

Figure S12. Separation of various chloride and nitrate rare-earth pairs.

10. Stripping efficiency over time

The stripping efficiency of Ho^{3+} ions from Fe_3O_4(TMS-EDTA) was measured after different contact times with the stripping solution (HCl solution) at pH 2.5.

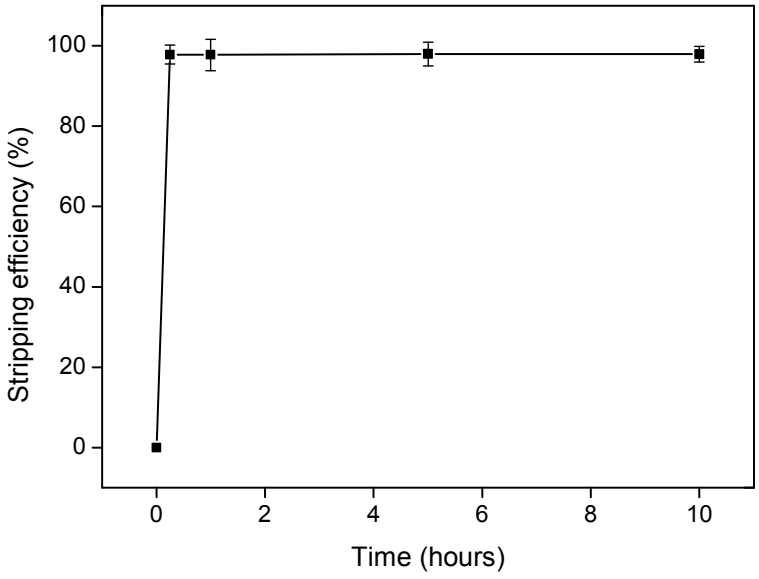

Figure S13. Influence of time on stripping efficiency.

11. Position of Y^{3+} in the separation series.

The position of Y^{3+} in the lanthanide series is known to vary depending on the separation system. *Figure S14* shows that for this system Y^{3+} behaves similarly to Nd^{3+} (EF =1) which is in agreement with previous observations for EDTA.

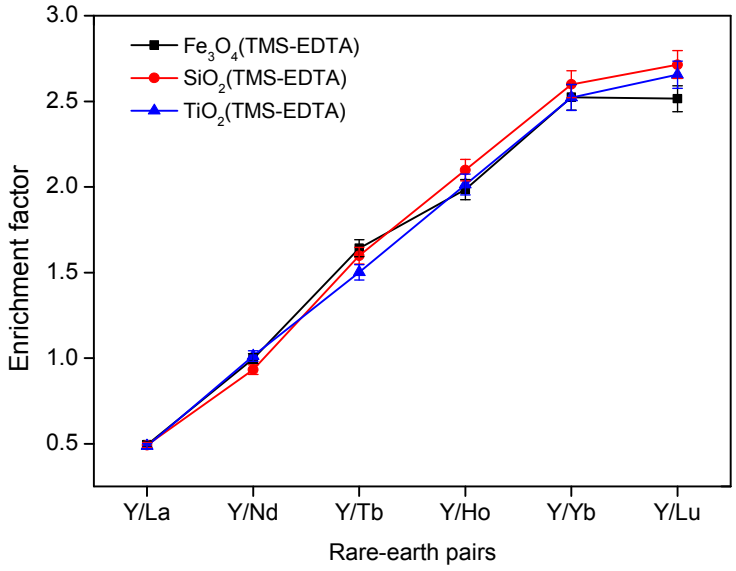

Figure S14. Separation of Y^{3+} / Ln^{3+} rare-earth pairs (pH 6.5) by three different EDTA-functionalized nanoparticles. The data points are ordered by increasing enrichment factor.

12. Additional separation experiments

Large differences in enrichment factors for different nanoparticles were only found for rare-earth pairs containing lanthanum, possibly because this is the only ion that is large enough to trigger the selectivity due to the density of EDTA groups on the surface. For other ions (e.g. Pr^{3+} and Lu^{3+}) the difference is much smaller as shown in Figure S15 and Figure S16. Note that EDTA has an inherent selectivity towards the heavier (smaller) lanthanide ions, so that any selectivity arising from the difference in surface density should be large enough compared to the inherent selectivity, otherwise it would not be observable.

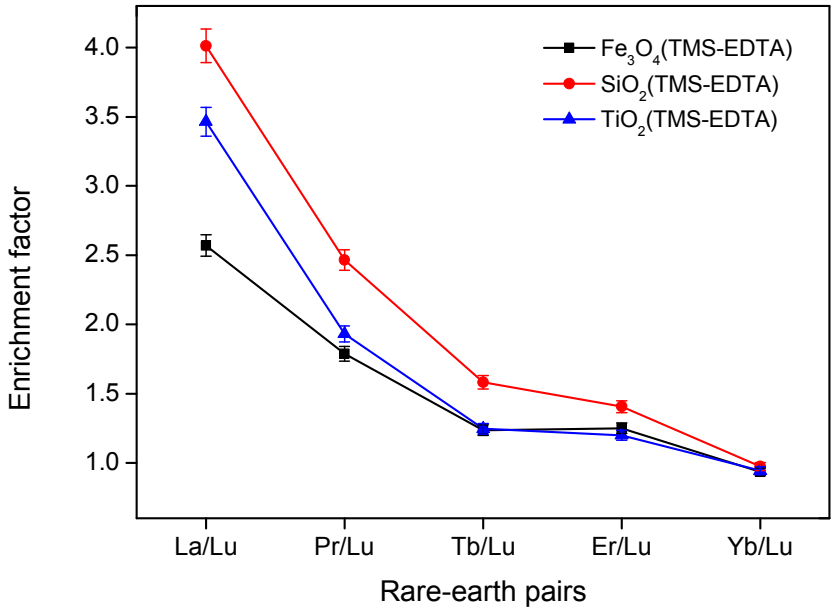

Figure S15. Separation of Ln^{3+} / Lu^{3+} (pH 6.5) by different nanoparticles functionalized with TMS-EDTA. The rare-earth pairs are ordered by decreasing difference in ionic radii from left to right.

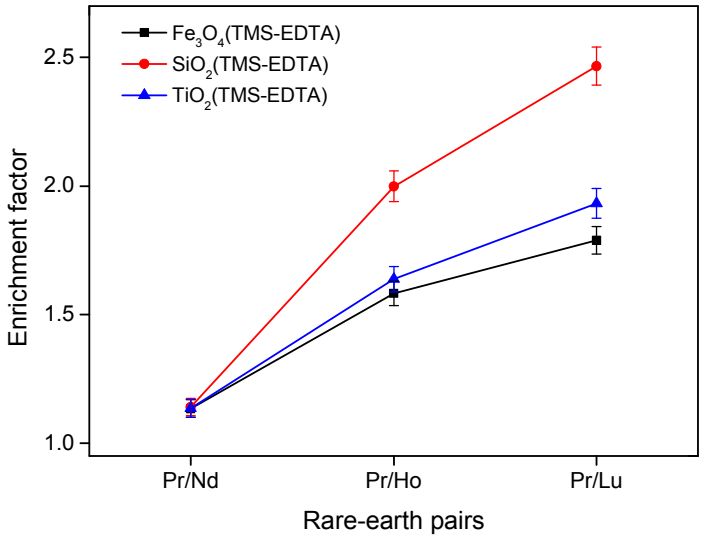

Figure S16. Separation of Pr^{3+}/Ln^{3+} (pH 6.5) by different nanoparticles functionalized with TMS-EDTA. The rare-earth pairs are ordered by increasing difference in ionic radii from left to right.